Received 18 December 2021; accepted 16 January 2022. Date of publication 25 January 2022; date of current version 22 February 2022.
The review of this article was arranged by Editor S. Reggiani.

Digital Object Identifier 10.1109/JEDS.2022.3145797

Enhancement of Breakdown Voltage in p-GaN Gate AlGaN/GaN HEMTs With a Stepped Hybrid GaN/AlN Buffer Layer

YUAN WANG[1], SHENGDONG HU[1], JINGWEI GUO[1], HAO WU[1,2], TAO LIU[1], AND JIE JIANG[1]

1 School of Microelectronics and Communication Engineering, Chongqing University, Chongqing 400030, China
2 Chongqing Engineering Laboratory of High Performance Integrated Circuits, Chongqing University, Chongqing 400044, China

CORRESPONDING AUTHOR: S. HU (e-mail: hushengdong@hotmail.com)

This work was supported in part by the National Natural Science Foundation of China under Grant 62174017; in part by the Natural Science Foundation Project of CQ CSTC under Grant cstc2020jcyj-msxmX0243; and in part by the Fundamental Research Funds for the Central Universities under Grant 2020CDJ-LHZZ-024.

ABSTRACT A novel p-GaN gate AlGaN/GaN high electron mobility transistor (HEMT) structure with a stepped hybrid GaN/AlN buffer layer (S-HEMT) is proposed and simulated by the Sentaurus TCAD in this paper. A stepped hybrid GaN/AlN buffer layer is adopted and the step is near the interface of the gate and drain. First, the breakdown voltage (*BV*) of the proposed S-HEMT is significantly improved with the introduction of a stepped hybrid GaN/AlN buffer layer, which can effectively modulate the electric field distributions along the channel. Second, the AlN buffer layer below the stepped GaN buffer has a large band offset and a strong polarization, which results in a much lower leakage current and a better carrier confinement. Consequently, the *BV* of the proposed S-HEMT will be improved at no expense of the specific on-resistance ($R_{on,sp}$). Compared with those of the conventional p-GaN gate AlGaN/GaN HEMT on the same gate-to-drain distance of 12 μm, a higher *BV* of 1781 V and FOM of 0.72 GW/cm^2 are obtained for the proposed S-HEMT, which are both about five times. The proposed S-HEMT exhibits the potential and advantage in high power electronic applications.

INDEX TERMS AlGaN/GaN HEMT, p-GaN, breakdown voltage, stepped hybrid GaN/AlN buffer.

I. INTRODUCTION

Gallium nitride (GaN)-based high electron mobility transistors (HEMTs) have been widely applied in high-power and high-frequency areas, owing to its excellent performances such as high breakdown electric field, high-electron mobility and good thermal stability [1]–[4]. For power devices, improving the breakdown voltage (*BV*) and reducing the specific on-resistance ($R_{on,sp}$) are the primary research targets [5]–[10]. Recently, the p-GaN gate technology has become one of the most promising methods to obtain normally-off GaN HEMTs to meet the fail-safe operation and the simply gate drive topology [11]–[12]. Based on the p-GaN gate AlGaN/GaN HEMTs, some new technologies have been proposed and applied to obtain a high *BV* and lower $R_{on,sp}$. Field plate (FP) technique is a usual method to enhance *BV* by means of electric field modulation effect [13]–[16]. Super junction (SJ) technology for GaN-based V-HFET [17]–[18] could decrease $R_{on,sp}$ by modulating the doping concentration. Duan *et al.* proposed a depletion-mode AlGaN/GaN HEMTs with a partial GaN cap, which applied the electric field modulation effect to reshape the surface electric field and two dimensional electronic gas (2DEG) distributions [19]. A novel p-GaN HEMT with a hybrid AlGaN buffer is proposed to improve the *BV* and decrease the $R_{on,sp}$, which can effectively modulate the electric field distribution in the channel and the buffer [20]. Recently, the AlN buffer layers is routinely employed to improve the confinement of 2DEG and make the electric field redistribution, which would further improve the *BV* because of its large bandgap energy of 6.2 eV and high polarization field [21]–[24]. Most of the researches are based on the surface electric field modulation, while few focus on the buffer.

In this paper, a novel p-GaN gate AlGaN/GaN HEMT structure with a stepped hybrid GaN/AlN layer (S-HEMT) is proposed in this paper. The study of the device is emphasized

This work is licensed under a Creative Commons Attribution 4.0 License. For more information, see https://creativecommons.org/licenses/by/4.0/

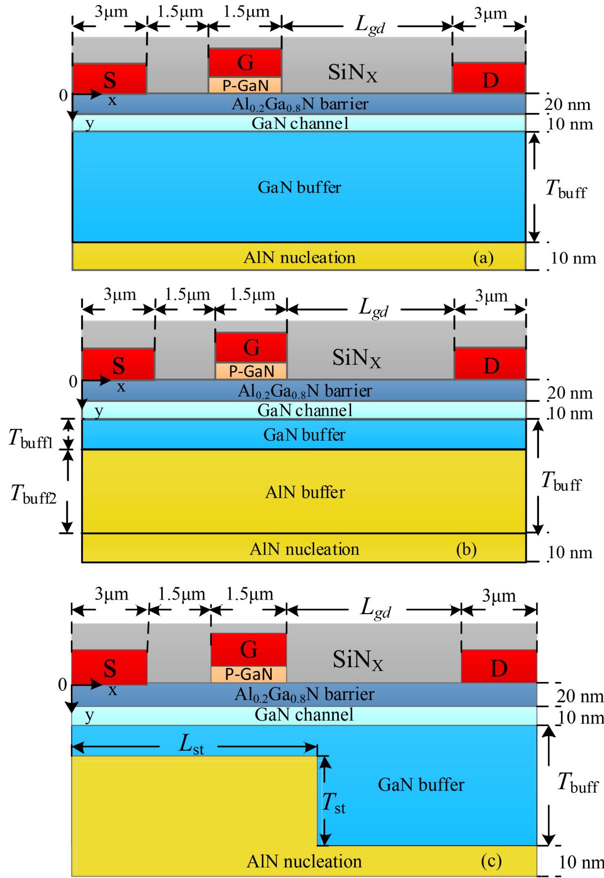

FIGURE 1. Schematic cross sections of (a) the C-HEMT, (b) the H-HEMT, and (c) the S-HEMT.

on increasing the *BV* at no expense of $R_{on,sp}$. The stepped hybrid GaN/AlN buffer layer is introduced to cause the electric field reshaped along the channel, resulting in a higher *BV*. Moreover, the leakage current is effectively lower by the AlN buffer layer below the stepped GaN buffer, further improving the *BV*. The main parameters of the proposed device will be optimized by the Sentaurus TCAD. The *BV* and the figure of merit (FOM $= BV^2/R_{on,sp}$) for the proposed device structure are much higher than those the conventional p-GaN gate AlGaN/GaN HEMT.

II. STRUCTURE AND MECHANISM

The schematic cross-sections of the conventional p-GaN gate AlGaN/GaN HEMT with GaN buffer layer (C-HEMT), the p-GaN gate AlGaN/GaN HEMT with the hybrid GaN/AlN buffer layer (H-HEMT), and the proposed p-GaN gate AlGaN/GaN HEMT with the stepped hybrid GaN/AlN buffer layer (S-HEMT) are shown in Fig. 1 (a), (b), and (c), respectively. In the proposed S-HEMT, a stepped hybrid GaN/AlN buffer layer is adopted and the interface of step is set between gate and drain. For the three devices, the thickness of the AlGaN barrier layer (T_{bar}), the GaN channel layer (T_{ch}) and the buffer layer (T_{buff}) are 20 nm, 10 nm, and 2 μm, respectively. The gate length (L_g), the source length (L_s) and the drain length (L_d) are 1.5, 3, and 3 μm. The thickness of the p-GaN layer (T_{p-GaN}) and the AlN nucleation (T_{nuc}) are 100 nm and 10 nm, respectively. For the proposed S-HEMT, the gate-drain distance (L_{gd}), the length (L_{st}) and thickness (T_{st}) of the stepped GaN buffer layer will be optimized. In addition, the sum of the thickness of the GaN buffer (T_{buff1}) and the AlN buffer layer (T_{buff2}) in the H-HEMT is always equal to the T_{buff}, and the T_{buff2} is equal to the T_{st}. The main structure parameters for the three devices are given in the Table 1.

TABLE 1. Main structure parameters in simulation.

Parameters	Value
Length of source electrode, L_s (μm)	3
Length of gate electrode, L_g (μm)	1.5
Length of drain electrode, L_d (μm)	3
Gate-to-source distance, L_{gs} (μm)	1.5
Gate-to-drain distance, L_{gd} (μm)	7-12
Thickness of p-GaN layer, T_{p-GaN} (nm)	100
Thickness of AlGaN barrier, T_{bar} (nm)	20
Thickness of GaN channel, T_{ch} (nm)	10
Thickness of buffer, T_{buff} (μm)	2
Thickness of GaN buffer in the H-HEMT, T_{buff1} (μm)	0.1-0.7
Thickness of AlN buffer in the H-HEMT, T_{buff2} (μm)	1.3-1.9
Length of the stepped GaN buffer in the S-HEMT, L_{st}(μm)	6.4-6.8
Thickness of the stepped GaN buffer in the S-HEMT, T_{st}(μm)	1.3-1.9
Thickness of AlN nucleation, T_{nuc} (nm)	10
Length of source electrode, L_s (μm)	3

The fabrication process of the proposed S-HEMT can be similar with that of the reported the AlGaN/GaN HEMT with thick AlN buffer layer [21]. The AlGaN/GaN/AlN epitaxial structure is grown by metal-organic chemical vapor deposition (MOCVD) on sapphire substrate. Before growing the GaN buffer, the AlN buffer layer is partially etched by using BCl_3 plasma based reactive ion etching (RIE) at a low RF power. The key process steps for an etching of AlN buffer layer should be controlling the etching RF power value and rapid annealing process to reduce the addition induced defects. Ohmic contacts are defined and metalized by electron beam evaporation after selectively plasma-etching a p-GaN layer. The SiN passivation layer is deposited by plasma enhanced chemical vapor deposition (PECVD), and the gate foot is defined by E-beam lithography (EBL). While, the interface state between the buffer layer and transition layer has been considered in simulation, and the breakdown voltage is not affected by adjusting the trap concentration value of the interface state.

The Two-dimensional device simulations for the proposed devices in this paper are performed by using the Sentaurus TCAD tool. The mobility model is used based on the experimental measurement [21]. The piezoelectric polarization model is considered according to the experimental reports [25]. The Shockley-Read-Hall (SRH) recombination model, avalanche model, carrier tunneling model and no band gap narrowing model are also adopted in the simulation. Other material physical parameters are adopted according to the reports [26]–[27]. The normally-off p-GaN gate HEMT fabricated and measured by Zhang *et al.* [28] is

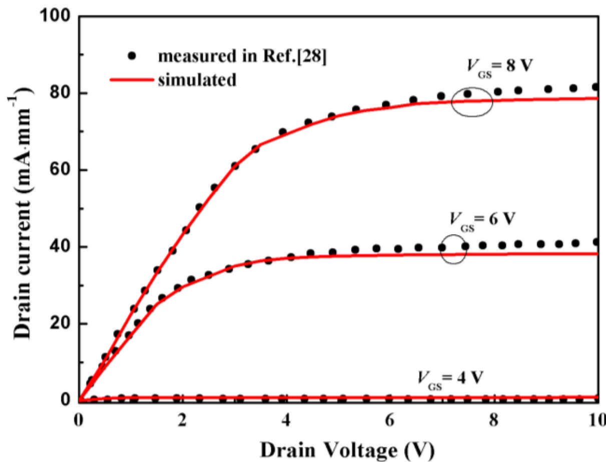

FIGURE 2. Experimental and simulated output characteristics for the normally-off p-GaN gate HEMT.

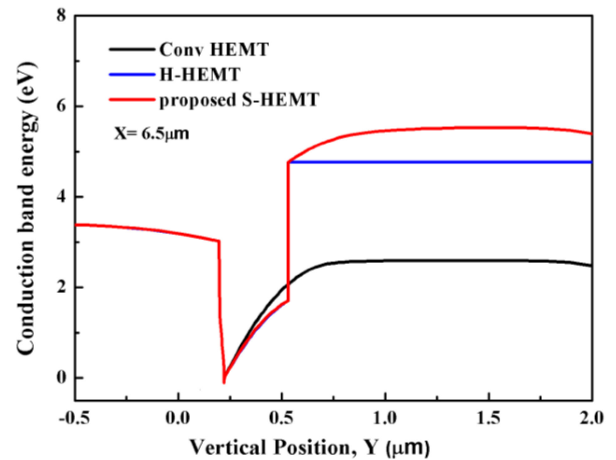

FIGURE 3. The conduction band diagrams of the C-HEMT, the H-HEMT and the proposed S-HEMT at X = 6.5 μm.

used to calibrate the simulation models and parameters. The normally-off p-GaN gate HEMT consists of a 4.3-μm-thick graded AlGaN buffer, a 100-nm-thick AlGaN channel and a gate-drain distance of 5μm. The simulated normally-off p-GaN gate HEMT has a threshold voltage of 4 V, which is consistent with the experimental result [28]. Fig. 2 shows the output characteristics of the experimental and simulated results for the normally-off p-GaN gate HEMT. The simulated results show great fitting well with the experimental results, demonstrating the accuracy of the simulation models. In simulation, the breakdown mechanism is usually avalanche breakdown caused by impact ionization. The impact ionization depends not only on the peak value of the electric field distribution, but also its shape near the peak [15], thus, if not specified, the breakdown voltage in this paper is defined as the drain voltage when the drain current reaches to 1×10^{-7} A/mm.

For the H-HEMT and S-HEMT, the buffer leakage current at the off-state is lower than the C-HEMT. The conduction band diagrams of the three kinds of devices at X = 6.5 μm are displayed in Fig. 3. It is obviously seen that the AlN buffer layer below the GaN buffer or the stepped GaN buffer has a larger band offset and a stronger polarization, which results in much lower leakage current and better carrier confinement for the devices. Then, the gate avalanche breakdown due to the rapid increase of electric field peak at the gate close to the drain is suppressed by the step buffer, therefore the depletion region is extended and the average lateral electric field between gate and drain is increased. All of these reasons result in a higher *BV* at off-state.

III. RESULTS AND DISCUSSION

Fig. 4 shows the on-state I-V characteristics for the C-HEMT, the H-HEMT and the proposed S-HEMT. As is shown in Fig. 4 (a), when the drain-source voltage V_{DS} is set as 0.1V, all of devices exhibit the same threshold voltage (V_{TH}) of about 1.1V, which is shown that the V_{TH} of the proposed S-HEMT has not been affected by the stepped hybrid GaN/AlN buffer layer. Fig. 4 (b) indicates the $I_{ds}-V_{ds}$ curves at V_{GS} is set to 3V for the C-HEMT, the H-HEMT and the proposed S-HEMT, a linear part of which is shown in the insert picture (V_{ds} ranges from 0V to 1V). The proposed S-HEMT exhibits slightly higher maximum drain current of 245 mA/mm compared with the H-HEMT of 244 mA/mm and the C-HEMT of 237 mA/mm, as is shown in Fig. 4 (b). From the insert picture, these three devices shows the same specific on-state resistance ($R_{on,sp}$) of 4.42 $m\Omega \cdot cm^2$.

Fig. 5 shows the equipotential lines distributions at breakdown for the C-HEMT, the H-HEMT and the proposed S-HEMT. It is obviously seen that the equipotential lines located at the gate close to the drain are more crowded for the C-HEMT than the other two devices. For the proposed S-HEMT, the stepped hybrid GaN/AlN buffer layer makes the equipotential lines which are located at the gate close to the drain more uniform owing to the redistribution of the electric field. Consequently, the proposed S-HEMT obtains a higher *BV* than the other two devices.

Fig. 6 shows the breakdown characteristics for the C-HEMT, the H-HEMT and the proposed S-HEMT with L_{gd} of 12 μm when the devices are turned off. The voltage of the V_{GS} is 0 V. It can be seen that the breakdown voltage for the proposed S-HEMT is 1781V, which is much higher than that of 319V for the C-HEMT and 1177V for the H-HEMT. Compared with the C-HEMT and the H-HEMT, the proposed S-HEMT shows higher breakdown voltage at no expense of the $R_{on,sp}$ and demonstrates its great superiority in high-power applications. The off-state buffer leakage current of the proposed S-HEMT and the H-HEMT are much lower than that of the C-HEMT, which results in an enhanced breakdown voltage at the off-state.

Fig. 7 shows the channel electric field distributions at off-state of V_{DS} = 1000V and $V_{DS} = BV$ for the H-HEMT and the proposed S-HEMT. As shown in Fig. 7 (a), the electric field crowding is near the gate edge for the two devices,

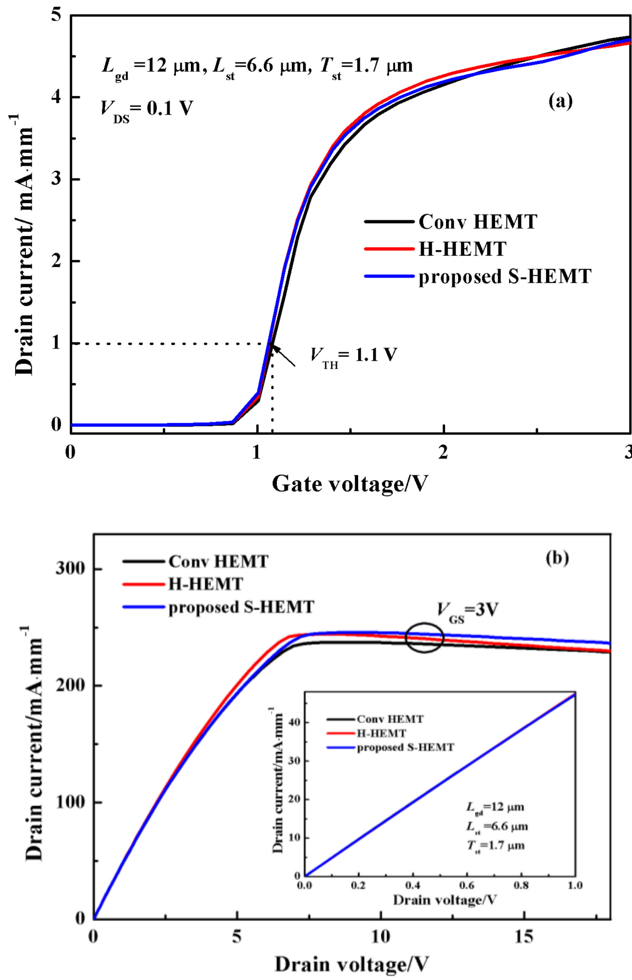

FIGURE 4. The on-state characteristics for the C-HEMT, the H-HEMT and the proposed S-HEMT, showing (a) transfer characteristics and (b) output characteristics.

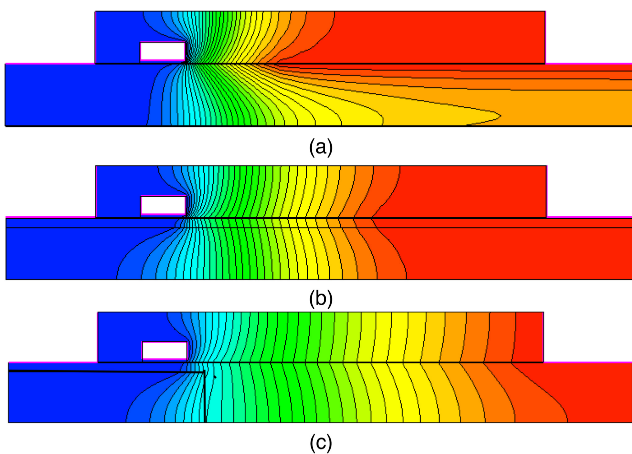

FIGURE 5. Equipotential lines distributions at breakdown for (a) the C-HEMT, (b) the H-HEMT and (c) the S-HEMT.

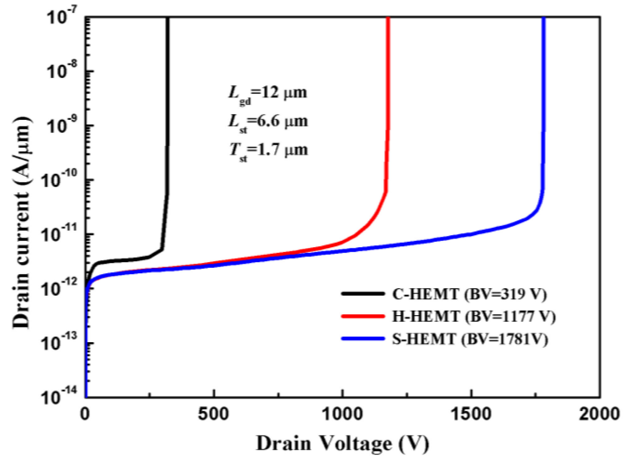

FIGURE 6. The breakdown characteristics for the C-HEMT, the H-HEMT and the proposed S-HEMT.

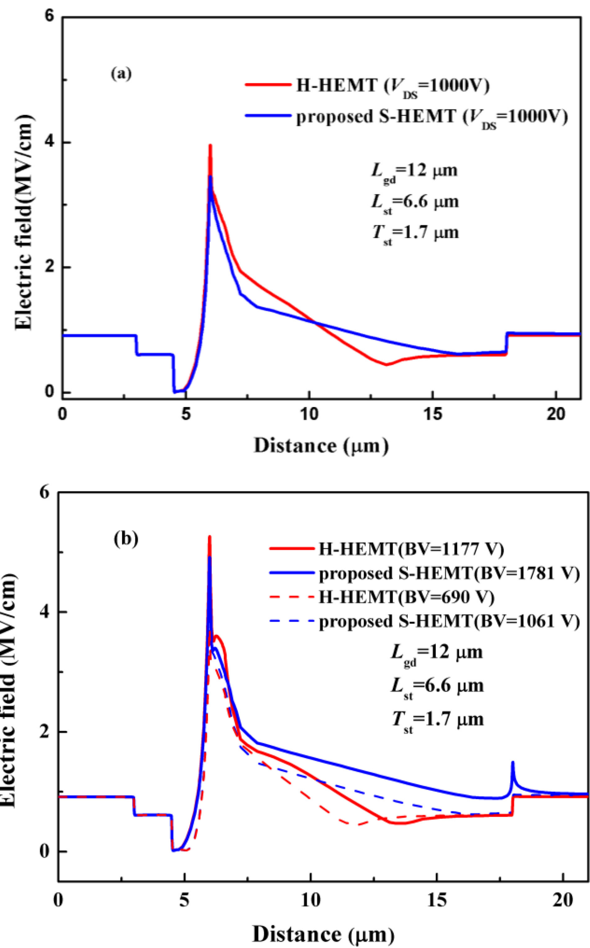

FIGURE 7. The electric field distributions along the GaN channels of the H-HEMT and the proposed S-HEMT at V_{DS} = 1000V (a) and V_{DS} = BV (b). The solid and dashed lines indicate that the breakdown criterion is based on the leakage current and the peak electric field, respectively.

but for the proposed S-HEMT the electric field peak near the gate edge is 3.4 MV/cm, which is lower than that of 4.0 MV/cm for the H-HEMT at a given V_{DS} of 1000V. It can be seen that the maximum electric field peak is reduced to a small value which lower than the critical electric field in the proposed S-HEMT due to the electric field modulation

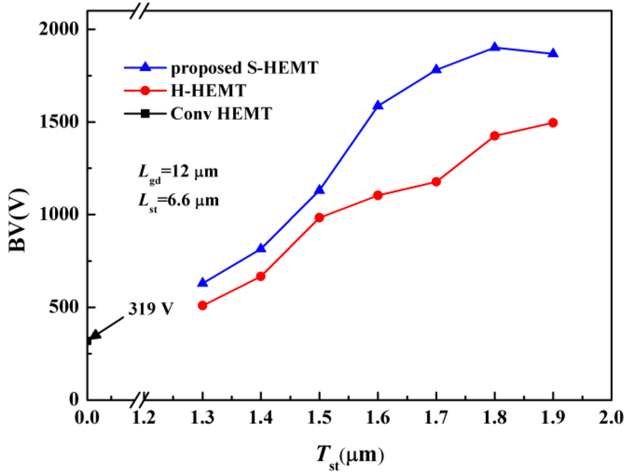

FIGURE 8. Breakdown voltages of the H-HEMT and the proposed S-HEMT versus T_{st}.

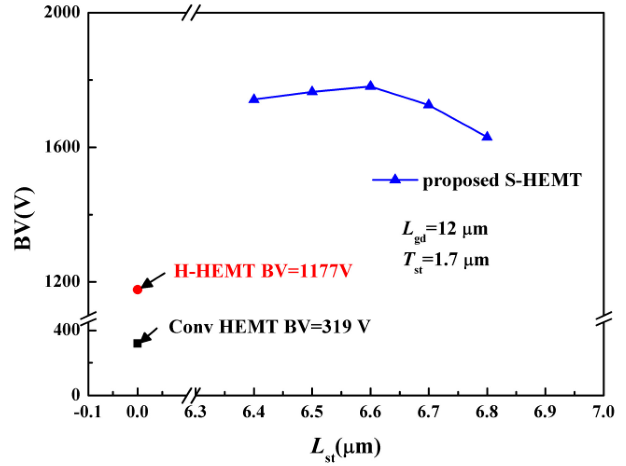

FIGURE 9. Breakdown voltages of the H-HEMT and the proposed S-HEMT versus L_{st}.

effect of the step structure. Therefore, when the device is breakdown, as can be seen in Fig. 7 (b), the gate to drain region can be further depleted and the average electric field is enhanced dramatically. Consequently, the *BV* of the proposed S-HEMT is increased. In order to make the analysis more comprehensive, the breakdown voltage is also defined as the drain voltage when the peak electric field value reaches to 3.7 MV/cm. The channel electric field distributions of the H-HEMT and the proposed S-HEMT are indicated by dashed lines in Fig. 7 (b). The breakdown voltage of the proposed S-HEMT is 1061V, which is also much higher than that of 690 V for the H-HEMT.

Breakdown voltages for the proposed S-HEMT and the H-HEMT with different thickness of the stepped GaN buffer have been simulated to obtain the optimal value of T_{st}, where the T_{buff2} is always equal to the T_{st}. Fig. 8 shows the *BV* for the H-HEMT and the proposed S-HEMT with different T_{st}. As shown in Fig. 8, the *BV* of the proposed S-HEMT increases with an increasing of T_{st} at $T_{st} < 1.8$ μm due to the reduced off-state buffer leakage current, while decreases at $T_{st} > 1.8$ μm. And then the *BV* of the H-HEMT increases linearly with an increasing of T_{st} because of premature breakdown happened at the gate close to the drain. While compared with the H-HEMT, the highest percentage increase in *BV* for the proposed S-HEMT is 51.3% at $T_{st} = 1.7$ μm. In consider of this reason, the optimal value of T_{st} is identified as 1.7 μm.

The length of the stepped GaN buffer has been optimized to obtain a higher *BV*. Fig. 9 shows the *BV* for the proposed S-HEMT with different L_{st}. It is obviously seen that the *BV* of the proposed S-HEMT increases slowly and then decreases rapidly with an increasing of L_{st}, owing to the redistributed electric field along the GaN channel. The highest breakdown voltage (1781V) is obtained with L_{st} of 6.6μm. Therefore, the optimal value of L_{st} for the proposed S-HEMT with L_{gd} of 12μm and T_{st} of 1.7μm is identified as 6.6μm.

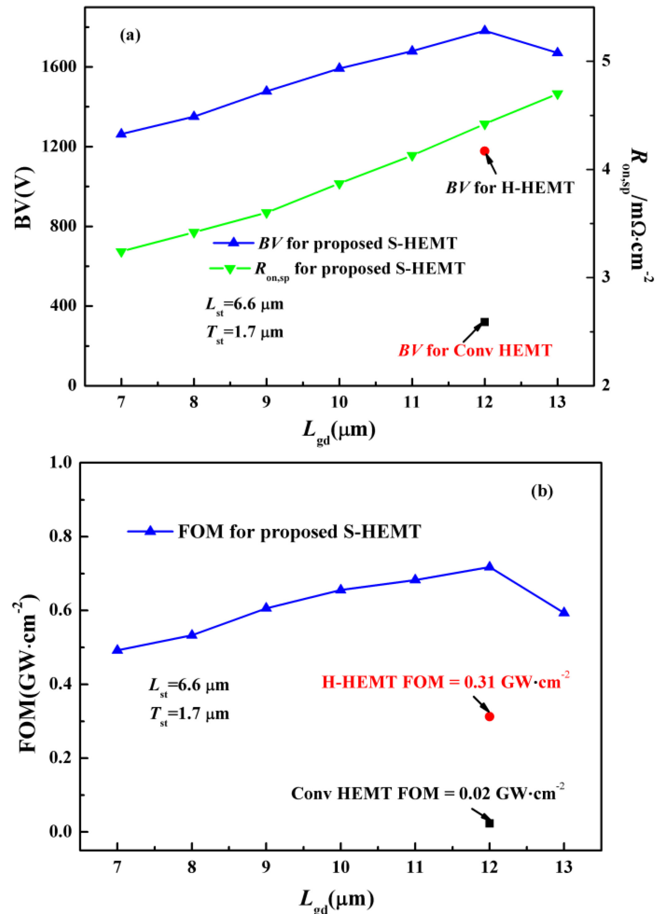

FIGURE 10. The *BV*, $R_{on,sp}$ (a) and calculated FOM (b) for the proposed S-HEMT versus L_{gd}.

For the proposed S-HEMT, the optimal value of L_{st} is always same when the gate-to-drain distance is increased. Breakdown voltages for the proposed S-HEMT with different L_{gd} have been simulated with L_{st} of 6.6 μm and T_{st} of 1.7 μm. Fig. 10 shows the *BV*, $R_{on,sp}$ (a) and calculated

FOM (b) for the proposed S-HEMT versus L_{gd}. It is visibly seen that the BV of the proposed S-HEMT increases first and then decreases, and the BV reaches up to a maximum value of 1781 V when $L_{gd} = 12$ μm. Meanwhile, the $R_{on,sp}$ increases linearly with an increasing of L_{gd}. In Fig. 10 (b), the value of FOM maintains a higher value than 0.2 GW/cm^2 when L_{gd} increases from 7 μm to 13μm. Significantly, the FOM of the proposed S-HEMT is as high as 0.72 GW/cm^2, which is much higher than that of 0.02 GW/cm^2 for the C-HEMT and 0.31 GW/cm^2 for the H-HEMT.

IV. CONCLUSION

A novel p-GaN gate AlGaN/GaN HEMTs with a stepped hybrid GaN/AlN buffer Layer is proposed and optimized using the Sentaurus TCAD simulation tools in this paper. Systematical studies and analyses of the device performances have been conducted, and L_{st}, T_{st} and L_{gd} have been optimized. The simulation results exhibits the remarkable improvement in BV of 1781V at no expense of $R_{on,sp}$. The lower buffer leakage current and the redistributed electric field along the channel result in a higher BV at the off-state. Compared with the C-HEMT, the BV and FOM for the proposed S-HEMT with the same L_{gd} of 12μm are improved by 458% and 3500%, respectively. The proposed S-HEMT exhibits the potential in high power electronic applications.

REFERENCES

[1] T. Imada, M. Kanamura, and T. Kikkawa, "Enhancement-mode GaN MIS-HEMTs for power supplies," in *Proc. Int. Power Electron. Conf.*, Sapporo, Japan, 2010, pp. 1027–1033, doi: 10.1109/IPEC.2010.5542039.

[2] M. Alshahed *et al.*, "Low-dispersion, high-voltage, low-leakage GaN HEMTs on native GaN substrates," *IEEE Trans. Electron Devices*, vol. 65, no. 7, pp. 2939–2947, Jul. 2018, doi: 10.1109/TED.2018.2832250.

[3] Y.-F. Wu *et al.*, "30-W/mm GaN HEMTs by field plate optimization," *IEEE Electron Device Lett.*, vol. 25, no. 3, pp. 117–119, Mar. 2004, doi: 10.1109/LED.2003.822667.

[4] U. K. Mishra, P. Parikh, and Y.-F. Wu, "AlGaN/GaN HEMTs-an overview of device operation and applications," *Proc. IEEE*, vol. 90, no. 6, pp. 1022–1031, Jun. 2002, doi: 10.1109/JPROC.2002.1021567.

[5] C. Wang *et al.*, "E-mode p-n junction/AlGaN/GaN (PNJ) HEMTs," *IEEE Electron Device Lett.*, vol. 41, no. 4, pp. 545–548, Apr. 2020, doi: 10.1109/LED.2020.2977143.

[6] Y. C. Choi, M. Pophristic, H. Cha, B. Peres, M. G. Spencer, and L. F. Eastman, "The effect of an Fe-doped GaN buffer on off-state breakdown characteristics in AlGaN/GaN HEMTs on Si substrate," *IEEE Trans. Electron Devices*, vol. 53, no. 12, pp. 2926–2931, Dec. 2006, doi: 10.1109/TED.2006.885679.

[7] H. Hanawa, H. Onodera, A. Nakajima, and K. Horio, "Numerical analysis of breakdown voltage enhancement in AlGaN/GaN HEMTs with a high-k passivation layer," *IEEE Trans. Electron Devices*, vol. 61, no. 3, pp. 769–775, Mar. 2014, doi: 10.1109/TED.2014.2298194.

[8] E. Bahat-Treidel, F. Brunner, O. Hilt, E. Cho, J. Wurfl, and G. Trankle, "AlGaN/GaN/GaN: C back-barrier HFETs with breakdown voltage of over 1 kV and low RON × A," *IEEE Trans. Electron Devices*, vol. 57, no. 11, pp. 3050–3058, Nov. 2010, doi: 10.1109/TED.2010.2069566.

[9] I. B. Rowena, S. L. Selvaraj, and T. Egawa, "Buffer Thickness contribution to suppress vertical leakage current with high breakdown field (2.3 MV/cm) for GaN on Si," *IEEE Electron Device Lett.*, vol. 32, no. 11, pp. 1534–1536, Nov. 2011, doi: 10.1109/LED.2011.2166052.

[10] B. Lu, E. L. Piner, and T. Palacios, "Schottky-drain technology for AlGaN/GaN high-electron mobility transistors," *IEEE Electron Device Lett.*, vol. 31, no. 4, pp. 302–304, Apr. 2010, doi: 10.1109/LED.2010.2040704.

[11] G. Greco, F. Iucolano, and F. Roccaforte, "Review of technology for normally-off HEMTs with p-GaN gate," *Mater. Sci. Semicond. Process.*, vol. 78, pp. 96–106, May 2018, doi: 10.1016/j.mssp.2017.09.027.

[12] Y. Qi *et al.*, "Effect of x-ray irradiation on threshold voltage of AlGaN/GaN HEMTs with p-GaN and MIS Gates," *Nanotechnol. Precis. Eng.*, vol. 3, no. 4, pp. 241–243, Dec. 2020.

[13] H. Xing, Y. Dora, A. Chini, S. Heikman, S. Keller, and U. K. Mishra, "High breakdown voltage AlGaN-GaN HEMTs achieved by multiple field plates," *IEEE Electron Device Lett.*, vol. 25, no. 4, pp. 161–163, Apr. 2004, doi: 10.1109/LED.2004.824845.

[14] Y. Dora, A. Chakraborty, L. Mccarthy, S. Keller, S. P. Denbaars, and U. K. Mishra, "High breakdown voltage achieved on AlGaN/GaN HEMTs with integrated slant field plates," *IEEE Electron Device Lett.*, vol. 27, no. 9, pp. 713–715, Sep. 2006, doi: 10.1109/LED.2006.881020.

[15] S. Karmalkar and U. K. Mishra, "Enhancement of breakdown voltage in AlGaN/GaN high electron mobility transistors using a field plate," *IEEE Trans. Electron Devices*, vol. 48, no. 8, pp. 1515–1521, Aug. 2001, doi: 10.1109/16.936500.

[16] T. Kabemura, S. Ueda, Y. Kawada, and K. Horio, "Enhancement of breakdown voltage in AlGaN/GaN HEMTs: Field plate plus high-k passivation layer and high acceptor density in buffer layer," *IEEE Trans. Electron Devices*, vol. 65, no. 9, pp. 3848–3854, Sep. 2018, doi: 10.1109/TED.2018.2857774.

[17] W. Mao *et al.*, "Low specific on-resistance GaN-based vertical heterostructure field effect transistors with nonuniform doping superjunctions," *Chin. Phys. B*, vol. 27, no.4, pp. 430–435, Apr. 2018, doi: 10.1088/1674-1056/27/4/047305.

[18] X. Luo *et al.*, "Ultralow specific on-resistance superjunction vertical DMOS with high-K dielectric pillar," *IEEE Electron Device Lett.*, vol. 33, no. 7, pp. 1042–1044, Jul. 2012, doi: 10.1109/LED.2012.2196969.

[19] B. Duan, L. Yang, Y. Wang, and Y. Yang, "Experimental results for AlGaN/GaN HEMTs improving breakdown voltage and output current by electric field modulation," *IEEE Trans. Electron Devices*, vol. 68, no. 5, pp. 2240–2245, May 2021, doi: 10.1109/TED.2021.3067865.

[20] Y. Liu, Q. Yu, and J. Du, "A novel high breakdown voltage and high switching speed GaN HEMT with p-GaN gate and hybrid AlGaN buffer layer for power electronics applications," *Chin. Phys. B*, vol. 29, no. 12, pp. 554–561, Dec. 2020, doi: 10.1088/1674-1056/abaee5.

[21] J.-G. Kim, C. Cho, E. Kim, J. S. Hwang, K.-H. Park, and J.-H. Lee, "High breakdown voltage and low-current dispersion in AlGaN/GaN HEMTs with high-quality AlN buffer layer," *IEEE Trans. Electron Devices*, vol. 68, no. 4, pp. 1513–1517, Apr. 2021, doi: 10.1109/TED.2021.3057000.

[22] S. Arulkumaran, T. Egawa, S. Matsui, and H. Ishikawa, "Enhancement of breakdown voltage by AlN buffer layer thickness in AlGaN/GaN high-electron-mobility transistors on 4 in. diameter silicon," *Appl. Phys. Lett.*, vol. 86, no. 12, 2004, Art. no. 123503, doi: 10.1063/1.1879091.

[23] S. Arulkumaran, M. Sakai, T. Egawa, H. Ishikawa, and T. Jimbo, "Improved DC characteristics of AlGaN/GaN high-electron-mobility transistors on AlN/sapphire templates," *Appl. Phys. Lett.*, vol. 81, no. 6, pp. 1131–1133, Aug. 2002, doi: 10.1063/1.1498874.

[24] I. Abid *et al.*, "High lateral breakdown voltage in thin channel AlGaN/GaN high electron mobility transistors on AlN/sapphire templates," *Micromachines*, vol. 10, no. 10, p. 690, Oct. 2019, doi: 10.3390/mi10100690.

[25] O. Ambacher *et al.*, "Two-dimensional electron gases induced by spontaneous and piezoelectric polarization charges in N- and Ga-face AlGaN/GaN heterostructures," *J. Appl. Phys.*, vol. 85, no. 6, pp. 3222–3233, Mar. 1999, doi: 10.1063/1.369664.

[26] J. Piprek *Semiconductor Optoelectronic Devices: Introduction to Physics and Simulation*. Santa Barbrara, CA, USA: Elsevier Sci., Jan. 2003.

[27] I. Vurgaftman, J. R. Meyer, and L. R. Ram-Mohan, "Band parameters for III-V compound semiconductors and their alloys," *J. Appl. Phys.*, vol. 89, no. 11, pp. 5815–5875, Jun. 2001, doi: 10.1063/1.1368156.

[28] L. Zhang *et al.*, "AlGaN-channel gate injection transistor on silicon substrate with adjustable 4–7-V threshold voltage and 1.3-kV breakdown voltage," *IEEE Electron Device Lett.*, vol. 39, no. 7, pp. 1026–1029, Jul. 2018, doi: 10.1109/LED.2018.2838542.